The influence of exchange of sensible heat with the earth's surface on the planetary flow[1]

By BO R. DÖÖS, *Institute of Meteorology, University of Stockholm and Swedish Meteorological and Hydrological Institute*

(Manuscript received January 22, 1962)

ABSTRACT

The exchange of sensible heat with the earth's surface is one of the most important external forces which influence the motion of the atmosphere. This is studied with the aid of a linearized model, where the heating is assumed to be proportional to the difference between the temperature of the air at the bottom of the atmosphere and the temperature of the underlying surface. Since the temperature of the air is one of the dependent variables, the heating is dependent on the motion. The vertical decrease of the heating is given by a power function.

Stationary disturbances on the zonal flow are evaluated for a simple temperature distribution of the ground which corresponds to conditions in middle latitudes in winter, which result from the effects of two continents and two oceans. The resulting horizontal distribution of the heat sources and sinks is evaluated. It is found that the positions of the heat sources are about 30° to the west of the temperature maximum of the underlying surface.

The influence of friction, the vertical variation of the heating and the zonal wind profile are studied separately.

The longitudinal variation of the heating along 45° N is compared with the normal sensible heat transfer in winter estimated from observations. Good agreement is obtained both regarding the magnitude of the heating and the phase difference between the heating and the ground temperature fields.

1. Introduction

The problem of taking into account non-adiabatic heating in theoretical studies of the behaviour of the large scale flow-pattern is indeed very important. Together with mountain and friction effects the non-adiabatic heating is one of the most important sources of error in numerical weather prediction. A number of investigations have been made in order to obtain information on how the large scale heat sources influence the steady state motion of the atmosphere. SMAGORINSKY (1953) has used a thermally active model to study this problem, where he also compared the results with the observed normals for the Northern Hemisphere. DE LISLE & HARPER (1961) studied the same problem for the Southern Hemisphere. In both these investigations the heat sources and sinks were geographically fixed.

Since the heating of the atmosphere in reality is no doubt a function of the motion itself, the results obtained with such models may be misleading. MINTZ (1958*a*) stressed this point and has also made an attempt to put this idea into effect (MINTZ, 1958*b*). This is also done in an investigation by KUO & NORDÖ (1958), in which the quasi non-divergent equations were integrated over the Northern Hemisphere. The effects of the average radiational heating and cooling, the heat exchange between the atmosphere and its lower boundary, and the turbulent heat transfer were included.

However, it is difficult from studies of this type to obtain knowledge of how the different types of non-adiabatic heating influence the

[1] The research reported here has been sponsored by the Geophysics Research Directorate, AFCRL, AFRD of the Air Research and Development Command, USAF, through its European Office.

motion. It is therefore still of interest to use simple baroclinic models, with the aid of which the various forms of heating can be investigated with particular emphasis on the interplay between the heating and the motion.

When considering the steady state perturbations of the zonal flow on the planetary scale, there are chiefly three types of heating that influence the motion: heating due to condensation or evaporation (Q_p), turbulent exchange of heat with the earth's surface (Q_c) and heating due to radiation (Q_r). There is no doubt that, of these three types of heating, radiation has the least influence on the motion. It is true that the magnitude of this radiational heating is relatively large, but its variance is quite small. This is clearly demonstrated by CLAPP (1961) in an evaluation of the normal winter heating from sea level to 5.5 km due to radiation at all wavelengths. In the winter the other two heating processes (Q_p and Q_c) are by and large of equal importance. Both their magnitude and horizontal variation are fairly similar. In addition to the fact that both Q_p and Q_c are dependent on the motion, they are also mutually dependent on each other. For instance, heating due to exchange with the earth's surface may lead to convection, which in turn may lead to condensation. This at least partly explains the strong correlation between the horizontal distribution of these two heating fields.

In the present investigation we are interested in the effect of the non-adiabatic heating due to Q_c only. For this reason we cannot expect to obtain a close similarity between the results and observed conditions. The main purpose is here to aim at obtaining a fuller knowledge of how the transfer of sensible heat from the ground to the atmosphere influences the motion and vice versa. The heating function we shall make use of is similar to the one used by MINTZ (1958*b*). We have thus assumed Q_c to be proportional to the difference between the temperature of the air at the surface and the ground. The stationary disturbances on the zonal flow are thus controlled by the temperature distribution of the ground, which is chosen to resemble the temperature-field of the ground at middle latitudes, as caused by the effect of two oceans and two continents in winter. We shall also calculate the resulting horizontal distribution of the heat sources and sinks.

2. The fundamental equations

The fundamental equations we shall make use of in the study of this problem are the equations of vorticity and continuity, the first law of thermodynamics and the hydrostatic equation. In the x, y, p-coordinate system these equations read:

$$\frac{\partial \zeta}{\partial t} + \mathbf{v} \cdot \nabla (\zeta + f) + \omega \frac{\partial \zeta}{\partial p} = -(f+\zeta) \operatorname{div} \mathbf{v} + \frac{\partial \omega}{\partial y}\frac{\partial u}{\partial p} - \frac{\partial \omega}{\partial x}\frac{\partial v}{\partial p}, \tag{1}$$

$$\operatorname{div} \mathbf{v} + \frac{\partial \omega}{\partial p} = 0, \tag{2}$$

$$\frac{\partial}{\partial t}\left(\frac{\partial z}{\partial p}\right) + \mathbf{v} \cdot \nabla \left(\frac{\partial z}{\partial p}\right) + \sigma\omega = -\frac{R}{c_p g}\frac{Q(T,p)}{p}, \tag{3}$$

$$\frac{\partial z}{\partial p} = -\frac{RT}{gp}, \tag{4}$$

where ζ is the relative voricity, $\mathbf{v}$ the horizontal velocity vector which has the components u and v, ω the vertical p-velocity, ∇ the horizontal gradient operator, $\mathbf{k}$ the vertical unit vector, $f = 2\Omega \cdot \sin\varphi$ the Coriolis parameter, z the height of a pressure surface, R the gas constant for dry air, c_p the specific heat for dry air at constant pressure, g the acceleration of gravity, Q the rate of heat gained or lost per unit mass and unit time, T the temperature and σ the static stability defined by

$$\sigma = -\frac{1}{g\varrho\theta}\frac{\partial\theta}{\partial p} = \frac{\partial^2 z}{\partial p^2} + \frac{1}{\varkappa p}\frac{\partial z}{\partial p}, \tag{5}$$

where θ is the potential temperature and $\varkappa$ the ratio of the specific heat at constant pressure and constant volume.

We have thus four equations (1)–(4), which is one less than the number of dependent variables u, v, ω, z and T. However, one more equation will be furnished in connection with the discussion of the assumptions we shall make.

3. General assumptions

The following general assumptions are proposed:

(*a*) The motion is in geostrophic equilibrium.

(*b*) The motion is stationary.

(c) The non-linear effects can be neglected.
(d) The non-adiabatic heating is a function of the motion.
(e) The static stability is constant.
(f) The twisting term can be neglected.

In addition to eqs. (1)–(4) we have of course also the divergence equation. However, we shall make use of the assumption (a) that the motion is in geostrophic equilibrium. As a fifth equation we thus have

$$\mathbf{v} = -\frac{g}{f}\nabla z \times \mathbf{k}. \tag{6}$$

The assumptions (b) and (c) imply that we are going to consider infinitesimal stationary perturbations superimposed on a zonal current. We therefore introduce the following new variables:

$$u = U(p) + u'(x, y, p),$$

$$v = v'(x, y, p),$$

$$\omega = \omega'(x, y, p),$$

$$z = Z_0(y, p) + z'(x, y, p),$$

$$T = T_0(y, p) + T'(x, y, p),$$

where the primed variables represent the disturbed flow produced by the heating. The geostrophic wind components then read:

$$u = -\frac{g}{f}\frac{\partial Z_0}{\partial y} - \frac{g}{f}\frac{\partial z'}{\partial y}, \tag{7}$$

$$v = \frac{g}{f}\frac{\partial z'}{\partial x}. \tag{8}$$

The geostrophic vorticity will be approximated by

$$\zeta = \frac{g}{f}\nabla^2 z'.$$

We next consider the term in the thermodynamic equation (3) which represents the non-adiabatic heating (assumption (d)). The following expression for the turbulent heat exchange of heat with the earth's surface has been found fairly reliable by several authors in connection with climatological calculations of turbulent heat exchange over water surfaces

$$q = A V_s (T_g - T_s), \tag{9}$$

where q is the transfer of heat per unit time and unit area, A is a constant, V_s the wind speed, T_s the temperature of the air and T_g the temperature of the underlying surface. For a detailed discussion of this formula reference is made to Budyko (1956).

Over the continents the conditions regarding the exchange of sensible heat are quite different. The main reason for this is that the conductive capacity is much less there. Priestly (1959) has pointed out that it is a difference of the conductivity rather than the heat capacity which dominates the conductive capacity or the ability to conduct the heat away from the interface. This is quite well illustrated by Table 1, where the thermal properties of some typical surface substances are shown. The table is obtained from Petterssen (1959) and is a summary of values collected from different authors by Priestly (1957). We notice particularly that the conductive capacity of stirred water (oceans) is considerably larger than the corresponding values for solid materials. We see that over the oceans there must be a tendency for the air to adapt its temperature to the ocean surface, while over the continents it is

Table 1. *Physical properties of different media.*
(Cal–c.g.s. units)

Substance	Heat capacity[a] (ϱc)	Conductive capacity ($\varrho c\sqrt{K_T}$)	Conductive capacity (typical)
New snow	0.03	0.002	0.002
Old snow	0.22	0.012	0.01
Dry sand	0.3	0.011	
Wet sand	0.4	0.04	0.04
Sandy clay (15 % water)	0.59	0.036	
Organic soil	0.57	0.04	
Granite rock	0.5	0.02	
Ice	0.45	0.05	
Still water	1.0	0.039	
Stirred water	1.0	0.32–17	10
Still air	0.0003	0.0001	—
Stirred air	0.0003	0.01–0.1	0.1

[a] c is the specific heat and K_T the thermal diffusivity. For solid substances the molecular value is used and for fluids the eddy value.

more natural to expect that the ground adapts its temperature to the air. In spite of this we shall for simplicity only use one type of heating function (9).

In the present study we shall moreover make the assumption that the heating decreases with decreasing pressure according to a power-function. We thus have the following formula for the rate of heating per unit mass

$$Q = A V_s (T_g - T_s)\left(\frac{p}{p_s}\right)^r, \tag{10}$$

where r is a constant. Regarding the temperature of the ground we prescribe that its horizontal variation is represented by

$$T_g = T_{0g} + \tau_0 \sin kx \sin ly, \tag{11}$$

where $k = 2\pi/L_x$ and $l = 2\pi/L_y$, L_x and L_y being the wavelengths of the variation of the ground temperature in the x- and y-directions respectively and τ_0 the amplitude.

With the aid of the hydrostatic equation (4) we obtain the following expression for the temperature of the air at the surface.

$$T_s = -\frac{g p_s}{R}\left(\frac{\partial z}{\partial p}\right)_s = -\frac{g p_s}{R}\left(\frac{\partial Z_0}{\partial p}\right)_s - \frac{g p_s}{R}\left(\frac{\partial z'}{\partial p}\right)_s. \tag{12}$$

Making use of (11) and (12), the expression for Q (10) can be written

$$Q = A V_s \left[T_{0g} + \tau_0 \sin kx \sin ly + \frac{g p_s}{R}\left(\frac{\partial Z_0}{\partial p}\right)_s + \frac{g p_s}{R}\left(\frac{\partial z'}{\partial p}\right)_s\right]\left(\frac{p}{p_s}\right)^r. \tag{13}$$

It is here natural to restrict ourselves to consider the case when the air and the ground are in thermal equilibrium averaged along the x-axis (latitude).

Thus
$$T_{0g} - T_{0s} = -\frac{g p_s}{R}\left(\frac{\partial Z_0}{\partial p}\right)_s. \tag{14}$$

After linearization we obtain the final form of the expression for the non-adiabatic heating

$$Q = K\left[\tau_0 \sin kx \sin ly + \frac{g p_s}{R}\left(\frac{\partial z'}{\partial p}\right)_s\right]\left(\frac{p}{p_s}\right)^r, \tag{15}$$

where the coefficient $A V_s$ has been replaced by K.

The assumption (e) regarding the static stability is fairly well justified in the middle and lower part of the troposphere. It certainly simplifies the mathematical procedure.

Finally we have the assumption regarding the twisting term (f). An estimate of how justified this is may be obtained by comparing the orders of magnitude of the divergence term and the twisting term in the vorticity equation. After linearization these two terms read

$$f\frac{\partial \omega'}{\partial p} \quad \text{and} \quad \frac{\partial \omega}{\partial y}\frac{dU}{dp}.$$

The orders of magnitude of these terms may be represented by the scale quantities. We can then write the two terms

$$f\frac{\omega}{p^*/2} \quad \text{and} \quad \frac{\omega}{S}\frac{V}{p^*},$$

where p^* is the pressure which corresponds to the depth of the troposphere and S the characteristic horizontal distance in the y-direction. Taking the ratio of these two terms gives

$$\frac{\text{twisting term}}{\text{divergence term}} \sim \frac{V}{2fS}.$$

If we take S as small as 10 degrees of latitude $\sim 10^6$ m, $V = 20$ msec^{-1} and $f = 10^{-4}$ sec^{-1}, this ratio becomes 10^{-1}, indicating that the neglect of the twisting term is not a too severe assumption.

After making use of the assumptions (a) to (f) and eliminating the dependent variables u', v', ω' and T', we arrive at the following third order partial differential equation in z',

$$\frac{\partial}{\partial x}\left[\frac{\partial^2 z'}{\partial p^2} + \left(\frac{g\sigma}{f^2}\frac{\beta}{U} - \frac{1}{U}\frac{d^2 U}{dp^2}\right)z' + \frac{g\sigma}{f^2}\nabla^2 z'\right] = -\frac{RK}{c_p g p_s U}\left[\tau_0 \sin kx \sin ly + \frac{g p_s}{R}\left(\frac{\partial z'}{\partial p}\right)_s\right]\frac{d}{dp}\left(\frac{p}{p_s}\right)^{r-1}. \tag{16}$$

We assume that the solution to this equation can be written in the form

$$z' = [Z_1(p) \sin kx + Z_2(p) \cos kx] \sin ly. \tag{17}$$

Introducing this expression for z' in (16) gives a system of two ordinary differential equations for Z_1 and Z_2 which is combined into one equation by making use of the new dependent variable

$$Z = Z_1 + iZ_2. \tag{18}$$

At the same time we replace the independent variable p by the non-dimensional variable

$$P = \frac{p}{p_s}. \tag{19}$$

With (17), (18) and (19) we then obtain the following ordinary differential equation from (16)

$$\frac{d^2Z}{dP^2} + \left(\frac{\beta s^2}{U} - \frac{1}{U}\frac{d^2U}{dP^2} - \gamma^2\right)Z$$
$$= i\frac{U_0}{U}\left[\mu\left(\frac{dZ}{dP}\right)_s + a\right]\frac{d}{dP}P^{r-1}, \tag{20}$$

where

$$\left.\begin{aligned} s^2 &= \frac{g\sigma p_s^2}{f^2}, \\ a &= \frac{RK\tau_0}{kc_pgU_0}, \\ \mu &= \frac{K}{kc_pU_0}, \\ \gamma &= s\sqrt{k^2+l^2}. \end{aligned}\right\} \tag{21}$$

U_0 is an arbitrary constant with the dimension of a velocity.

4. Boundary conditions

As the upper boundary condition we prescribe

$$\omega = 0 \quad at \quad P = 0. \tag{22}$$

At the bottom of the atmosphere ($P = 1$), defined as the top of the friction layer, we assume that the vertical velocity w is determined by ground friction. Thus we have

$$\omega = \frac{dp}{dt} = \frac{\partial p}{\partial t} + \mathbf{v}\cdot\nabla p - g\varrho w \quad \text{at} \quad P = 1. \tag{23}$$

The first two terms on the right-hand side vanish because of assumptions (b) and (a) respectively. For estimating the vertical velocity we make use of the following expression given by Charney & Eliassen (1949).

$$\omega = -g\varrho_s\left(\frac{2K^*}{f}\right)^{\frac{1}{2}} \sin\alpha\cos\alpha\,\zeta_g \quad \text{at} \quad P = 1, \tag{24}$$

where ϱ_s is the density of the air, K^* the eddy viscosity coefficient, α the angle between surface wind and surface isobars, and ζ_g the geostrophic vorticity.

In order to express these two boundary conditions in terms of the dependent variable z we make use of the thermodynamic equation which, after introducing the assumptions (a) to (e), reads

$$\omega' = -\frac{1}{\sigma p_s}\left\{U\frac{\partial}{\partial x}\frac{\partial z'}{\partial P} - \frac{dU}{dP}\frac{\partial z'}{\partial x}\right.$$
$$\left. + \frac{RK}{c_pg}\left[\tau_0 \sin kx \sin ly + \frac{g}{R}\left(\frac{\partial z'}{\partial P}\right)_s\right] P^{r-1}\right\}. \tag{25}$$

Together with (17) and (18) we can now write the boundary conditions (22) and (24) as

$$\frac{dZ}{dP} - \frac{1}{U}\frac{dU}{dP}Z = 0 \quad \text{for} \quad r > 1, \tag{26a}$$

$$\frac{dZ}{dP} - i\mu\frac{U_0}{U}\left(\frac{dZ}{dP}\right)_s - \frac{1}{U}\frac{dU}{dP}Z - ia\frac{U_0}{U} = 0$$
$$\text{for} \quad r = 1 \quad \text{at} \quad P = 0. \tag{26b}$$

$$\left(1 - i\mu\frac{U_0}{U}\right)\frac{dZ}{dP} - \left(\frac{1}{U}\frac{dU}{dP} + i\nu\frac{U_0}{U}\right)Z - ia\frac{U_0}{U}$$
$$= 0 \quad \text{at} \quad P = 1, \tag{27}$$

where a and μ are defined in (21) while

$$\nu = \frac{\sigma p_s^2 g^2}{U_0RT_sf}\left(\frac{2K^*}{f}\right)^{\frac{1}{2}}\frac{k^2+l^2}{k}\sin\alpha\cos\alpha. \tag{28}$$

5. Solutions

The equation to be solved for Z is (20) together with the boundary conditions (26) and (27). The type of this equation will depend on the assumption we make regarding the vertical variation of the main zonal wind U. If we make the common assumption that the wind varies linearly with respect to pressure, the equation will be of the confluent hypergeometric type. Although this type of equation is relatively extensively discussed in the literature, the numerical evaluation of the solution will be rather lengthy because of the form of the non-homogeneous term. In order to avoid this difficulty we have investigated the possibility of finding a wind profile which simplifies the equation but at the same time is realistic. A natural procedure is then to study the solutions to the differential equation in U

$$\frac{\beta s^2}{U}-\frac{1}{U}\frac{d^2U}{dP^2}=C, \tag{29}$$

where C is a constant. If this equation is satisfied, (20) is reduced to a differential equation which has constant coefficients.

The solutions to eq. (29) are

$$U=A\sin mP+B\cos mP+\frac{\beta s^2}{m^2}\quad\text{for}\quad C=m^2>0, \tag{30 a}$$

$$U=\frac{\beta s^2}{2}P^2+AP+B\quad\text{for}\quad C=0, \tag{30 b}$$

$$U=Ae^{nP}+Be^{-nP}-\frac{\beta s^2}{n^2}\quad\text{for}\quad C=-n^2<0. \tag{30 c}$$

The constants occurring in these different expressions for U can be determined so that a relatively realistic wind profile is obtained.

It is evident that the simplest form of wind profile to use is (30*b*). In this case the constants A and B get values such that we can write

$$U=\tfrac{1}{2}\beta s^2(P-\varepsilon)^2, \tag{31}$$

where ε is a non-dimensional constant. If we chose the arbitrary constant U_0 to be $\beta s^2/2$, we have

$$U=U_0(P-\varepsilon)^2. \tag{32}$$

A somewhat better agreement with observed conditions can be obtained if we make use of (30*a*). The drawback with this choice of wind profile is that the non-homogeneous term in eq. (20) becomes more complicated.

In addition to these two wind profiles we shall for comparison also solve the equation under the simplest assumption that the wind is independent of the pressure.

Regarding the vertical variation of the non-adiabatic heating we notice that the differential equation reduces to a homogeneous equation if $r=1$. Also the upper boundary condition assumes a special form in this case.

Because of this we shall distinguish between three different types of solutions to eq. (20)

I. $U=U_0(P-\varepsilon)^2,\ r=2.$

In this model the differential equation (20) becomes

$$\frac{d^2Z}{dP^2}-\gamma^2Z=\frac{i}{(P-\varepsilon)^2}\left[\mu\left(\frac{dZ}{dP}\right)_s+a\right]. \tag{33}$$

The boundary conditions are

$$\frac{dZ}{dP}+\frac{2}{\varepsilon}Z=0\quad\text{at}\quad P=0, \tag{34}$$

$$\left(1-\frac{i\mu}{(1-\varepsilon)^2}\right)\frac{dZ}{dP}-\left(\frac{2}{1-\varepsilon}+\frac{i\nu}{(1-\varepsilon)^2}\right)Z-\frac{ia}{(1-\varepsilon)^2}=0\quad\text{at}\quad P=1. \tag{35}$$

The solution is

$$\begin{aligned}Z=A&\left[e^{\gamma P}-\frac{\mu^2\gamma e^{\gamma}F'(1)}{H(1)}F(P)-i\frac{\mu\gamma e^{\gamma}}{H(1)}F(P)\right]\\&+B\left[e^{-\gamma P}+\frac{\mu^2\gamma e^{-\gamma}F'(1)}{H(1)}F(P)\right.\\&\left.+i\frac{\mu\gamma e^{-\gamma}}{H(1)}F(P)\right]-[\mu F'(1)+i]\frac{a}{H(1)}F(P),\end{aligned} \tag{36}$$

where

$$\begin{aligned}F(P)=&\cosh[\gamma(\varepsilon-P)]\left\{\log(\varepsilon-P)+\sum_{n=1}^{\infty}\frac{[\gamma(\varepsilon-P)]^{2n}}{2n\,(2n)!}\right\}\\&+\sinh[\gamma(\varepsilon-P)]\sum_{n=1}^{\infty}\frac{[\gamma(\varepsilon-P)]^{2n-1}}{(2n-1)\,(2n-1)!},\end{aligned} \tag{37}$$

$$H(1)=1+[\mu F'(1)^2]. \tag{38}$$

A prime denotes here a differentiation with respect to P.

II *a*. $U=U_0(P-\varepsilon)^2,\ r=1.$

The differential equation (20) reduces in this model to

$$\frac{d^2Z}{dP^2}-\gamma^2Z=0. \tag{39}$$

The boundary conditions are:

$$\frac{dZ}{dP}-\frac{i\mu}{\varepsilon^2}\left(\frac{dZ}{dP}\right)_s+\frac{2}{\varepsilon}Z-\frac{ia}{\varepsilon^2}=0 \quad \text{at} \quad P=0, \tag{40}$$

$$\left(1-\frac{i\mu}{(1-\varepsilon)^2}\right)\frac{dZ}{dP}-\left(\frac{2}{1-\varepsilon}+\frac{i\nu}{(1-\varepsilon)^2}\right)Z-\frac{ia}{(1-\varepsilon)^2}=0 \quad \text{at} \quad P=1. \tag{41}$$

The solution is

$$Z=Ae^{\gamma P}+Be^{-\gamma P}. \tag{42}$$

Since the non-homogeneous term vanishes in this case, it is very simple to make use of the wind profile of the type (30 *b*). We prefer to write this function in a slightly different form.

II *b*. $U=U_1 \sin(mP+\delta)+2\frac{U_0}{m^2}, \quad r=1.$

The differential equation (20) reads now

$$\frac{d^2Z}{dP^2}+(m^2-\gamma^2)Z=0. \tag{43}$$

The boundary conditions are

$$\left(U_1\sin\delta+2\frac{U_0}{m^2}\right)\frac{dZ}{dP}-i\mu U_0\left(\frac{dZ}{dP}\right)_s-(mU_1\cos\delta)Z-iaU_0=0 \quad \text{at} \quad P=0, \tag{44}$$

$$\left(U_1\sin(m+\delta)+2\frac{U_0}{m^2}-i\mu U_0\right)\frac{dZ}{dP}-(mU_1\cos(m+\delta)+i\nu U_0)Z-iaU_0=0 \quad \text{at} \quad P=1. \tag{45}$$

The solution is

$$\begin{aligned} Z&=Ae^{\Gamma_1 P}+Be^{-\Gamma_1 P} && \text{for} \quad \Gamma_1^2=\gamma^2-m^2>0,\\ Z&=AP+B && \text{for} \quad \gamma^2-m^2=0,\\ Z&=A\sin\Gamma_2 P+B\cos\Gamma_2 P && \text{for} \quad \Gamma_2^2=m^2-\gamma^2>0. \end{aligned} \tag{46}$$

III. $U=U^*=$ const., $r=2$.

The differential equation (20) becomes

$$\frac{d^2Z}{dP^2}-\left(\gamma^2-2\frac{U_0}{U^*}\right)Z=i\frac{U_0}{U^*}\left[\mu\left(\frac{dZ}{dP}\right)_s+a\right]. \tag{47}$$

The boundary conditions are

$$\frac{dZ}{dP}=0 \quad \text{at} \quad P=0, \tag{48}$$

$$\left(1-i\mu\frac{U_0}{U^*}\right)\frac{dZ}{dP}-i\nu\frac{U_0}{U^*}Z-ia\frac{U_0}{U^*}=0 \quad \text{at} \quad P=1. \tag{49}$$

The solution is

$$Z=A\left(e^{\Gamma_1 P}-\frac{i\mu}{\Gamma_1}\frac{U_0}{U^*}e^{\Gamma_1}\right)+B\left(e^{-\Gamma_1 P}+\frac{i\mu}{\Gamma_1}\frac{U_0}{U^*}e^{-\Gamma_1}\right)-\frac{ia}{\Gamma_1^2}\frac{U_0}{U^*},$$

$$\text{for} \quad \Gamma_1^2=\gamma^2-2\frac{U_0}{U^*}>0, \tag{50 a}$$

$$Z=\frac{\frac{a}{2}\frac{U_0}{U^*}\left(i-\mu\frac{U_0}{U^*}\right)}{1+\mu^2\left(\frac{U_0}{U^*}\right)^2}P^2+AP+B$$

$$\text{for} \quad \gamma^2-2\frac{U_0}{U^*}=0, \tag{50 b}$$

$$Z=A\left(\cos\Gamma_2 P-\frac{i\mu}{\Gamma_2}\frac{U_0}{U^*}\sin\Gamma_2\right)+B\left(\sin\Gamma_2 P+\frac{i\mu}{\Gamma_2}\frac{U_0}{U^*}\cos\Gamma_2\right)+\frac{ia}{\Gamma_2^2}\frac{U_0}{U^*} \quad \text{for} \quad \Gamma_2^2=2\frac{U_0}{U^*}-\gamma^2>0. \tag{50 c}$$

6. Results

In the numerical evaluation of the solutions we shall use the following values for the parameters and constants. The parameters which have different values in the various models are given in Table 2.

TABLE 2.

Model	U (m sec^{-1})	r	τ_0 (°C)	F(10^{-6} sec^{-1})
I *a*	14.5 (P–1.55)^2	2	10	1.4
I *b*	14.5 (P–1.55)^2	2	10	2.8
II *a*	14.5 (P–1.55)^2	1	6.67	1.4
II *b*	17.7 sin (0.745–1.39P) + 15	1	6.67	1.4
III *a*	15	2	10	1.4
III *b*	10	2	10	1.4

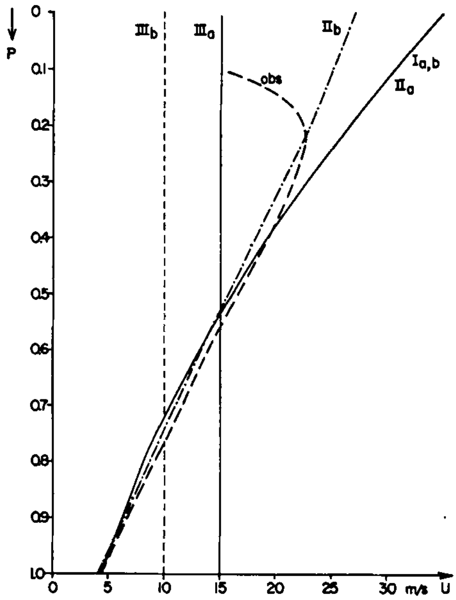

Fig. 1 *a*.

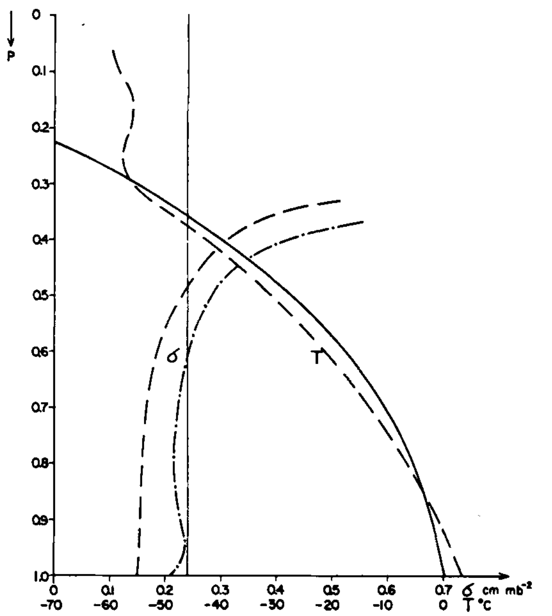

Fig. 1 *b*.

FIG. 1*a*. The vertical variation of the mean wind in the different models. The dashed curve shows the observed mean wind profile for the period December to February at 45° N (after CRUTCHER, 1959). FIG. 1*b*. The assumed value for the static stability and the corresponding vertical distribution of the temperature is represented by the solid lines. The dashed lines show the vertical distribution of the static stability and the temperature in the air mass between the polar front jet and the sub-tropical jet in January (after DEFANT & TABA, 1958). The dashed-dotted line gives the static stability in January averaged over 45 of the United States (after GATES, 1958).

where $$F = \frac{g}{RT_s}(2K^* f)^{\frac{1}{2}} \sin\alpha \cdot \cos\alpha. \qquad (51)$$

Common for all these models are

$$f = 1.03 \times 10^{-4}\,\mathrm{sec}^{-1}$$
$$\beta = 1.62 \times 10^{-13}\,\mathrm{cm}^{-1}\,\mathrm{sec}^{-1}$$
$$L_x = 14{,}100\ \mathrm{km} = 1.41 \times 10^{9}\,\mathrm{cm}$$
$$L_y = 5000\ \mathrm{km} = 5 \times 10^{8}\,\mathrm{cm}$$
$$K = 10^{2}\,\mathrm{erg\,gm}^{-1}\,{}^\circ\mathrm{K}^{-1}\,\mathrm{sec}^{-1}$$
$$\sigma = 0.24\ \mathrm{cm\,mb}^{-2}$$
$$p_s = 900\ \mathrm{mb}$$
$$T_s = 273^\circ\mathrm{K}$$
$$R = 2.87 \times 10^{6}\,\mathrm{erg\,gm}^{-1}\,{}^\circ\mathrm{K}^{-1}$$
$$c_p = 1.005 \times 10^{7}\,\mathrm{erg\,gm}^{-1}\,{}^\circ\mathrm{K}^{-1}$$
$$g = 981\ \mathrm{cm\,sec}^{-2}$$

Before we discuss the results obtained we shall make some comments regarding the choice of the values of the parameters. In the first model (I) an attempt is made to obtain a reasonable resemblance to observed conditions during the winter season. The models II and III are selected to make it possible to study the influence on the result of the vertical distribution of the non-adiabatic heating and the zonal wind profile.

If we first consider the choice of the parameters in model I, we notice that the assumed wind profile (cf. Fig. 1*a*) shows a relatively close agreement with the observed mean wind profile for the period December–February at 45° N (CRUTCHER, 1959). In the upper parts the deviation is of course considerable.

The parameters which determine the temperature field of the ground are given by the amplitude τ_0 of the deviation from the zonal mean temperature along 45° N and the wave lengths for τ in the latitudinal (L_x) and meridional directions (L_y) respectively. The value of L_x is chosen to be half the circumference of the latitude circle at 45° N. This corresponds approximately to the variation of the temperature of the ground along 45° N, where we have two maxima and two minima caused by the effect of the continents and the oceans. The assignment of values of the wave length L_y and

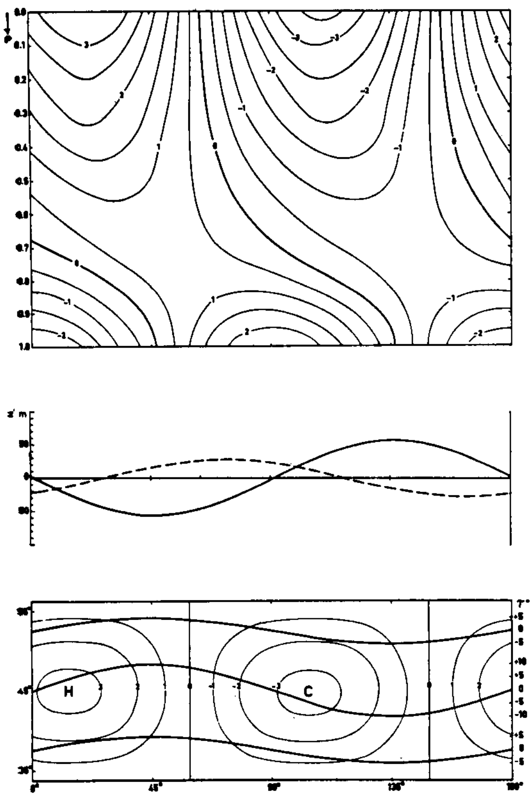

Fig. 2*a*.

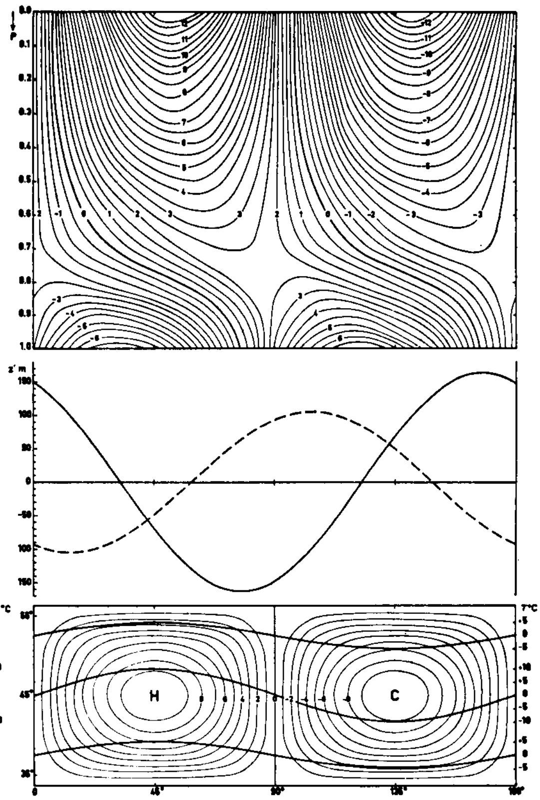

Fig. 2*b*.

FIG. 2*a*. Model I*a*, $\mu \neq 0$. In the upper part the perturbation meridional velocities in $\mathrm{m\,sec^{-1}}$ and in the middle part the perturbation height in m at $P = 1$ (solid line) and $P = 0.5$ (dashed line). These zonal sections are at the latitude (45°N) of maximum variation of the ground temperature. In the lower part of the figure the horizontal distribution of the deviation τ (°C) of the ground temperature from its zonal mean value (thick lines) and the rate of heating Q at $P = 1$ in the unit $\mathrm{erg\,mg^{-1}sec^{-1}} \times 10^{3}$ (thin lines). Parameters: $\varepsilon = 1.55$; $r = 2$; $\tau_0 = 10$°C; $F = 1.4 \times 10^{-6}\ \mathrm{sec^{-1}}$. FIG. 2*b*. Model I*a*, $\mu = 0$. See Fig. 2*a* for legend and parameters.

the amplitude τ_0 is more difficult. Agreement between observed and assumed conditions is uncertain, particularly on this point. In this connection it can be mentioned that the solution for the height change z' is directly proportional to τ_0. This makes it indeed simple to study the dependence of the solution on this parameter.

The assumption behind the choice of the parameter r which determines how fast the non-adiabatic heating decreases with decreasing pressure, is in approximate agreement with various investigations. WINSTON (1955), for example, found that the major part of the heating is in the layer below 700 mb but that the contribution in the layer 700 to 500 mb is by no means negligible.

In the expression for the non-adiabatic heating (15) we have also the coefficient K. The value for this constant has been set to 100 $\mathrm{erg\,gm^{-1}\,°K^{-1}sec^{-1}}$. Thus we see that a temperature difference of 10°C between the ground and the air close to the ground gives a heat transfer of 1000 $\mathrm{erg\,gm^{-1}sec^{-1}}$. The corresponding value for the heating per square centimeter is obtained by integration along the vertical:

$$Q_1 = \int_0^{p_s} Q\,\frac{dp}{g} = \frac{p_s}{g}\int_0^1 K\tau_0 P^r dP = \frac{p_s}{g} K\tau_0 \frac{P^{r+1}}{r+1}.$$

For $r = 2$

$$Q_1 = 0.306 \times 10^{6}\ \mathrm{erg\ cm^{-2}\ sec^{-1}}$$
$$= 631\ \mathrm{cal\ cm^{-2}\ day^{-1}}.$$

10 – 62173372

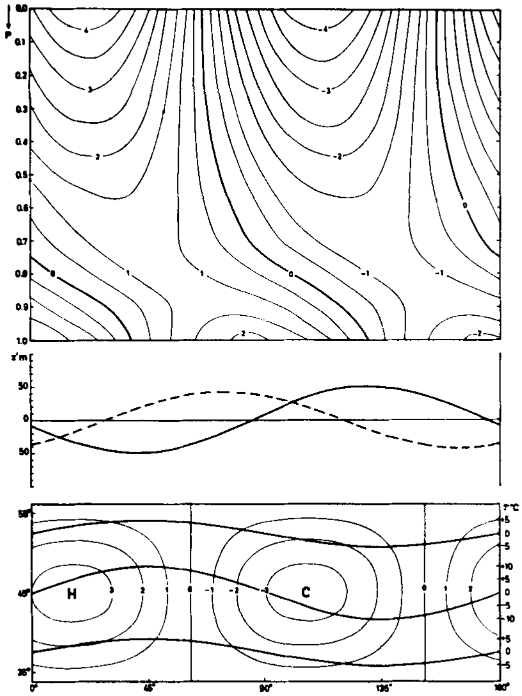

FIG. 3. Model Ib, $\mu \neq 0$. See Fig. 2a for legend. Parameters: $\varepsilon = 1.55$; $r = 2$; $\tau_0 = 10°C$; $F = 2.8 \times 10^{-6}$ sec^{-1}.

An estimate of the validity of the assumption that the expression for the static stability σ (5) is independent of the pressure can be obtained by studying Fig. 1b. The solid lines represent the value chosen for the static stability and the corresponding vertical distribution of the temperature. The dashed curve for the temperature is taken from DEFANT & TABA (1958) and represents the air mass between the polar front jet and the subtropical jet. The static stability is evaluated for this temperature distribution and is also shown in the figure by a dashed curve. The dashed-dotted curve is obtained from GATES (1958) and represents the stability as a function of pressure in January averaged over 45 of the United States. We notice that the observed static stability has a relatively small variation with pressure in the middle and lower troposphere. Higher up it increases rather rapidly.

The values of the parameters α and K^*, which determine the friction, are by no means certain. In order to facilitate comparison with other investigations we use expression (51), which is dependent on these parameters and is commonly used. All parameters which occur in this expression except α and K^* are given before. The two values for F which we shall use may then be obtained, for instance, by choosing:

Model Ia: $\alpha = 15°$, $K^* = 10^5$ cm^2 sec^{-1}
Model Ib: $\alpha = 22.5°$, $K^* = 2 \times 10^5$ cm^2 sec^{-1}

In this connection it can be mentioned that CHARNEY & ELIASSEN (1949) used the values $F = 2 \times 10^{-6}$ sec^{-1} and 4×10^{-6} sec^{-1} and SMAGORINSKY (1953) $F = 2 \times 10^{-6}$ sec^{-1}.

The results of the numerical evaluation of the solution for Model Ia is shown in Fig. 2a. In the middle part of the figure the height change z' is given as a function of x (longitude) for $P = 1$ (solid line) and for $P = 0.5$ (dashed line). The meridional wind component v' is shown in the upper part of the figure as a function of x and P. In the lower part of the figure the variation of the ground temperature is illustrated by thick lines. The thin lines represent here the non-adiabatic heating which is obtained by introducing the solution into the expression for Q (15).

For comparison we also evaluate the corresponding quantities for the case in which there is no influence of the motion on the non-adiabatic heating. This case is obtained by introducing $\mu = 0$ in the solution and the lower boundary condition, (35) to (38) (cf. Fig. 2b).

The other version of this model (Ib), where the friction is stronger, is shown in Fig. 3.

In model II the non-adiabatic heating has a different variation along the vertical. Here it decreases less rapidly with decreasing pressure. In addition we have here also changed the amplitude of the temperature deviation τ_0 in order to simplify a comparison with model Ia. τ_0 has been chosen so that the heating per square centimeter is the same in these two models for the case $\mu = 0$. The maximum heating as a function of pressure has been illustrated in Fig. 4 for both models Ia and IIa. For the case $\mu \neq 0$ solid lines are used and for $\mu = 0$, dashed lines. The results of model IIa are given in Figs. 5a and b.

In model IIb we have changed the vertical distribution of the mean wind (cf. Fig. 1a). Particularly in the upper layers it differs from the wind profile used in the models Ia, b and IIa. Finally we have model III, where we have no variation of the mean wind. The purpose of studying these models (IIb and IIIa, b) is merely to investigate the dependence of the resulting height change on the wind distribution with height.

7. Discussion

Before we turn to the discussion of the results, we shall comment on the solutions where there is no interplay between the motion and the heating, i.e. when $\mu = 0$, which has been evaluated for comparison. It is quite clear that this type of model must give results which are directly misleading if one still assumes that the heating is proportional to the temperature difference between the air at the ground and the underlying surface. We know from investigations regarding the geographical distribution of the heat sources and sinks, e.g. CLAPP (1961), that in mid-latitudes the maximum exchange of sensible heat with the earth's surface is found to the west of the maximum deviation of the mean ground temperature.

In the cases where $\mu = 0$, the heating term should thus represent the variation of the heating itself along the latitude 45° N. The drawback with this model is that the horizontal variation of the heating has to be prescribed. It is definitely an advantage to avoid this and instead prescribe the temperature of the ground. The heat sources should be determined by the motion. This has at least to some extent been attained in the present model ($\mu \neq 0$).

The discussion above is quite clearly illustrated by the results from the models I*a* (Figs. 2*a*, *b*) and II*a* (Figs. 5*a*, *b*) for which the solutions are evaluated for both $\mu \neq 0$ and $\mu = 0$. We thus find that when $\mu \neq 0$ in model I*a* the position of the heat source is about 30° to the west of the maximum value of the deviation of the ground temperature. The corresponding value in model II*a* is 25°. The intensity of the heating is naturally much less in the cases when $\mu \neq 0$, consequently the amplitude of the disturbances is smaller. However, the induced field of motion has the same phase relationship in relation to the longitudinal variation of the heating.

Regarding the effect of ground friction we can only hope that we have chosen the right order of magnitude for the parameter F. By comparing Fig. 2*a* (model I*a*: $F = 1.4 \times 10^{-6}$ sec^{-1}) and Fig. 3 (model I*b*: $F = 2.8 \times 10^{-6}$ sec^{-1}), we can at least get an estimate how dependent

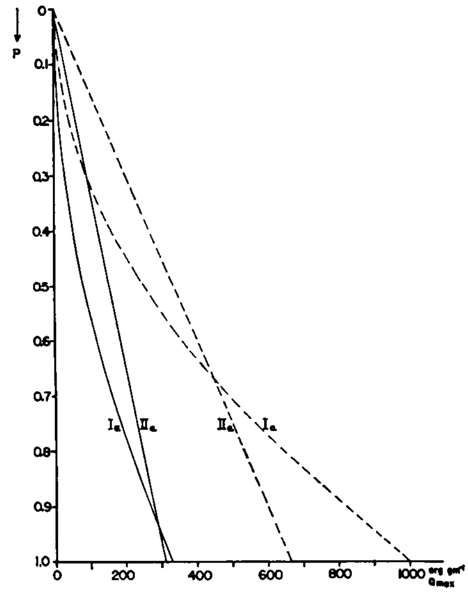

FIG. 4. The vertical variation of the maximum non-adiabatic heating. The solid lines represent the cases where $\mu \neq 0$, and the dashed lines where $\mu = 0$.

the solution is on this parameter. We observe that with increasing friction the amplitude of the disturbances decreases in the lower levels and increases in the upper levels. We also notice that the change of phase with height decreases with increasing friction. In addition to the quantities which occur in the parameter F the effect of friction is also dependent on the scale of the motion. A more detailed discussion of to what extent this is the case is found in an investigation of the stationary planetary waves by WIIN-NIELSEN (1961).

We next turn to discuss the influence of the parameter r which determines the vertical decrease of the non-adiabatic heating. By comparing the results of model I*a* (Figs. 2*a*, *b*: $r = 2$) and model II*a* (Figs. 5*a*, *b*: $r = 1$) we notice that if the heating decreases less rapidly with height (model II) the most rapid change of phase with height occurs higher up and that the disturbances are stronger in the lower levels and weaker in the upper levels. The positions of maximum heating and cooling are found further to the east in model II*a* ($\mu \neq 0$). The same is true for the troughs and ridges.

In the cases when $\mu = 0$ the total amount of heat added to the atmosphere is the same in both these models (the dashed lines in Fig. 4).

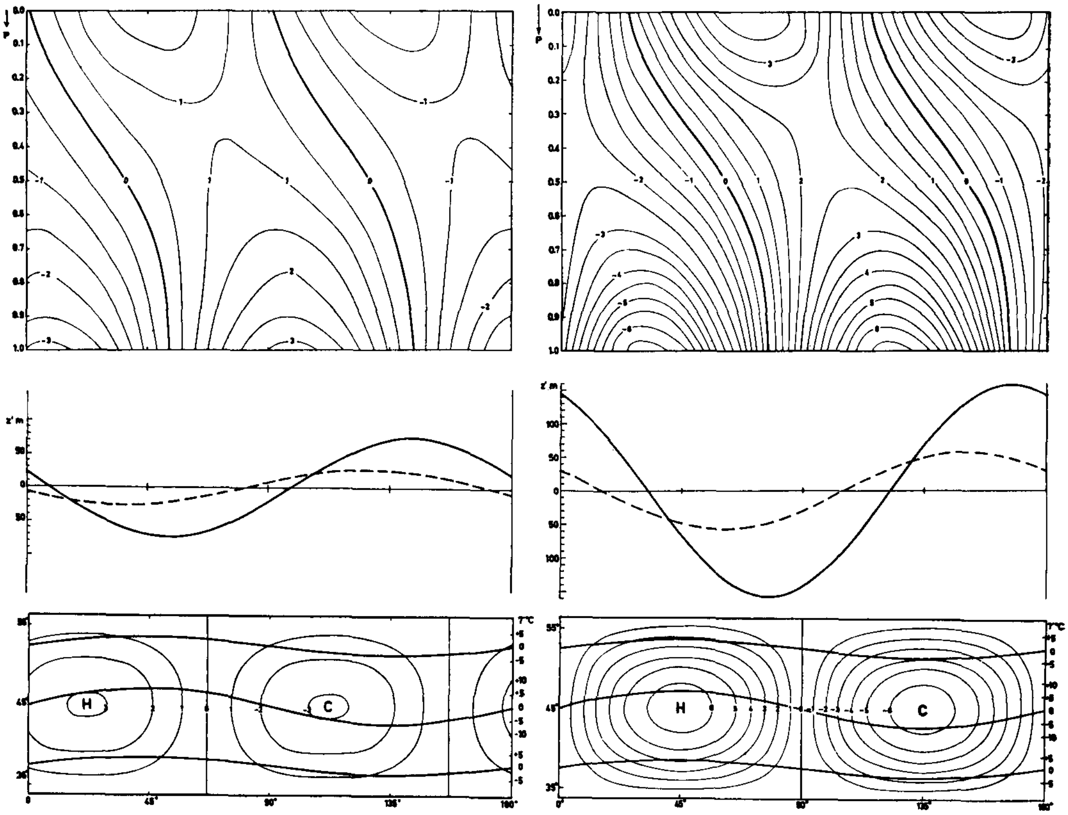

Fig. 5a. Fig. 5b.

FIG. 5a. Model IIa, $\mu \neq 0$. See Fig. 2a for legend. Parameters: $\varepsilon = 1.55$; $\tau_0 = 6\frac{2}{3}$°C; $F = 1.4 \times 10^{-6}$ sec^{-1}.
FIG. 5b. Model IIa, $\mu = 0$. See Fig. 2a for legend. Same parameters as in Fig. 5a.

For $\mu \neq 0$, however, we find that the heating is reduced to about one third in model Ia, while in model IIa the reduction is only about 50 per cent.

It is certainly also of interest to investigate how critical the choice of wind profile is on the results. This can at least partly be performed with the aid of the models IIb and IIIa, b. If we first consider model IIb, we notice that the only difference between IIa and IIb is the choice of wind profile (cf. Fig. 1a). The results obtained with these two models do not show any marked differences. The troughs and ridges have almost the same positions at $P = 1$, while the amplitude is about 10 per cent larger in model IIb. The phase shift with height over the entire interval ($P = 0$ to $P = 1$) is approximately the same but the most rapid change of phase with height occurs at lower levels in model IIb.

We next compare the results obtained with the models Ia and IIIa, b. Also here there is only a difference in the wind profile. As can be seen in Fig. Ia, the value for the wind in model IIIa ($U^* = 15$ m sec^{-1}) is chosen so that it is approximately the mean value with respect to pressure of the wind profile in model Ia. Here also the differences in the results (cf. Figs. 2a and 6) are relatively small.

These comparison indicate quite clearly that a small change in the wind profile does not change the results radically. However, if we reduce the mean wind sufficiently, resonance is reached, i.e. the wave length of the ground temperature distribution is equal to the stationary wave length of the baroclinic flow. In this case the induced field of motion will be quite different. In model IIIb the mean wind has such a value (10 m sec^{-1}) that we are very close to resonance. The results obtained with this model therefore differ considerably. Compared with model IIIa the amplitudes in the lower layers are much smaller and in the upper layers they are stronger. The troughs and ridges have a more westerly position (approximately 35°) and the phase shift with height is much less; however, there is still a westward tilt. We may also reach resonance by decreasing the term $l^2 + k^2$. The value of this term in model IIIa is 1.77×10^{-6} km^{-1}, while resonance occurs for 1.07×10^{-6} km^{-1}. In the present investigation $l = 2\sqrt{2}k$. We thus see that l is much more important than k. Since the value we have chosen for L_y (5000 km = 45° latitude) is considerably less than the value for which resonance occurs (L_y = 6717 km = 60.5° latitude for L_x = 14,100 km = 180° longitude at 45° N), the choice of this parameter is not too critical. The dependence of the solution on this parameter has been investigated and the result of this is in very close agreement with what Smagorinsky obtained. He used two different values of L_y (35° and 53.9° latitude), which quite safely can be regarded as the upper limit of this parameter.

Comparing the magnitude of the heating at $P = 1$ in model III, we find that the heating increases with increasing mean wind. Furthermore, we notice that the phase difference between the heating and ground temperature fields decreases with increasing wind. The physical explanation for this is obvious. The stronger the mean wind, the less time the air has to adapt its temperature to the ground temperature. Consequently, the temperature difference $T_g - T_s$ will be less reduced. The transfer of heat thus increases and reaches a maximum when U^* goes to infinity. It is to be emphasized that we have assumed the coefficient K in the heating function (10) to be constant.

8. Comparison with observations

It is evident that in an investigation of this type it is impossible to expect a close similarity between computed and observed conditions. However, it may still be of some interest to make some comparisons. For this purpose we have collected some of the results in Fig. 7, where we also show some observed quantities which are of interest in this connection. We have thus the observed height profiles of the 1000 mb and 500 mb normal maps along 45° N for January. In addition, the surface temperature of the oceans in February is shown, constructed from maps published by SVERDRUP (1952). Unfortunately it is impossible to obtain corresponding values for the continents. The normal winter heating, from sea level to 5.5 km, due to exchange of sensible heat with the earth's surface, has been obtained from CLAPP (1961), who has made a synthesis of several studies of the normal heat sources and sinks in winter. The sensible heat exchange over ocean areas was there obtained partly from JACOBS (1951) and partly from BUDYKO (1955). In Jacobs' estimate the sensible heat exchange is a function of the evaporation, the temperature gradient and the water vapour gradient near the sea surface, while Budyko used a formula (9) in which the heating is proportional to the product of the vertical temperature gradient and the wind. Over land

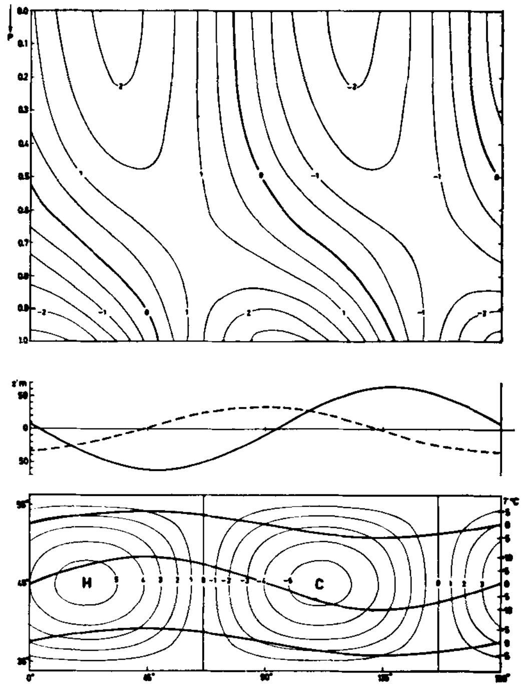

FIG. 6. Model IIIa, $\mu \neq 0$. See Fig. 2a for legend. Parameters: $U^* = 15$ m sec^{-1}; $r = 2$; $\tau_0 = 10$°C; $F = 1.4 \times 10^{-6}$ sec^{-1}.

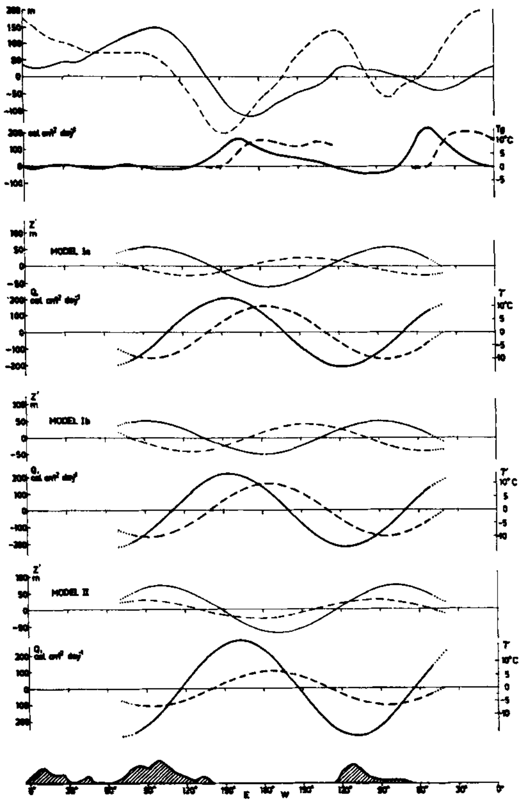

FIG. 7. At the top of the figure the observed profile of the 1000 mb surface (solid curve) and the 500 mb surface (dashed curve) along 45° N for the normal map of January. Below these curves are shown the surface temperature of the oceans in February at the same latitude (dashed curve) (after SVERDRUP, 1952). The solid curve here represents the normal winter heating, from sea level to 5.5 km, due to exchange of sensible heat with the earth's surface (after CLAPP, 1961).

In the lower parts of the figure the results from the models Ia, Ib and IIa are represented by the perturbation heights at $P = 1.0$ (solid curves) and $P = 0.5$ (dashed curves). The assumed variation of the ground temperature T_g for these three models are given by dashed curves and the computed total heating per square centimeter by solid curves.

areas the sensible heat exchange was obtained from the equation for heat balance of the land surface. We see that the estimated cooling over the continents is considerably smaller than the heating over the oceans. This is of course a direct consequence of the fact stated before that the conductive capacity is much less for solid materia. In order to facilitate the comparison between these observed quantities and our computed profiles we orient the latter so that the assumed temperature variation of the surface by and large coincides with the observed variation. Thus we place the τ curve in such a way that the positive value for τ corresponds to the surface temperature of the Pacific Ocean.

If we first consider the curves which represent the variation of the heating, we notice that the observed maxima are oriented about 25–30° to the west of the temperature maximum of the underlying surface. Approximately the same value for the phase difference is obtained in all three models represented in this figure. Regarding the magnitude of the maximum heating it is to be noted that the values estimated from observations refer to the layer below 5.5 km. However, the contribution of the heating in the models is relatively small above this level. Hence we conclude that the heating in the models Ia and Ib gives quite good agreement with the estimated values, while in model II the heating is too large.

Concerning the variation of the pressure surfaces we have no possibility of making a direct comparison with observed conditions, since we have only taken into account one of the effects which produce forced perturbations. We will therefore only make some general comments. The computed profiles (particularly model Ib) show a fairly good agreement with the observed profiles regarding the position of the troughs and ridges; the amplitudes, however, are much too small. This is not too surprising. In addition to the effect of the exchange of sensible heat we have in reality also other non-adiabatic effects, such as heating due to radiation and condensation or evaporation. The influence of the earth's topography is also quite important. In the region we consider in the first place (the Pacific Ocean) the heating due to evaporation or condensation is probably the most important of the neglected effects. It has here about the same horizontal distribution as the exchange of sensible heat. If this effect had been included in the model, it would have approximately resulted in a doubling of the amplitude of the disturbances, provided we had used the same vertical distribution of the heating.

In the case we chose to compare our results with the observed conditions in the Atlantic it is necessary to use a somewhat shorter wavelength in the longitudinal direction. It has been indicated before that the character of the solution is relatively independent of a small change in this parameter. With this in mind we can therefore conclude (cf. Fig. 7) that the agreement is quite good also here.

Acknowledgements

The author wishes to thank Professor Bert Bolin for his great interest and constructive criticism.

REFERENCES

Budyko, M. I., Ed., 1955, *Atlas of the Heat Balance.* (Atlas Teplovogo Balansa Glavnia Geofizicheskaia Observatoriia im A. I. Voeĭkova.) Leningrad, 41 pp.

Budyko, M. I., 1956, *The Heat Balance of the Earth's Surface.* (Translation prepared by Office of Technical Services, U.S. Department of Commerce: Teplovoĭ balans zemnoĭ poverkhnosti, Gidrometeorologischeskoe izdatel'stvo.) Leningrad, 256 pp.

Charney, J. G., and Eliassen, A., 1949, A numerical method for predicting the perturbations of the middle latitude westerlies. *Tellus,* **1**, pp. 38–55.

Clapp, P. F., 1961, Normal heat sources and sinks in the lower troposphere in winter. *Mon. Wea. Rev.,* **89**, pp. 147–162.

Crutcher, H. L., Ed., 1959, *Upper Wind Statistics of the Northern Hemisphere.* Issued by the Chief of Naval Operations.

Defant, Fr., and Taba, H., 1958, The breakdown of zonal circulation during the period January 8 to 13, 1956, the characteristics of temperature field and tropopause and its relation to the atmospheric field of motion. *Tellus,* **10**, pp. 430–450.

De Lisle, J. F., and Harper, J. F., 1961, A calculation of the effect of large-scale heat sources on southern hemisphere sub-tropical wind flow. *Tellus,* **13**, pp. 56–65.

Gates, W. L., 1958, *Static Stability Measures in the Atmosphere.* Scientific Report No. 3, Dynamical Weather Prediction Project. Univ. of California, Dept. of Meteorology, 22 pp.

Jacobs, W. C., 1951, The energy exchange between sea and atmosphere and some of its consequences. *Bull. Scripps Inst. Oceanogr.,* **6**, pp. 27–122.

Kuo, H. L., and Nordö, J., 1959, Integration of four-level prognostic equations over the hemisphere. *Tellus,* **11**, pp. 412–424.

Mintz, Y., 1958*a*, On the incorporation of non-adiabatic effects in numerical integration models for the study of the general circulation, in the dynamics of climate. *Proc. General Circulation Conf.* Institute for Advanced Study at Princeton, Oct. 1955.

Mintz, Y., 1958*b*, Design of some numerical general circulation experiments. *Bull. Res. Counc. of Israel,* **7 G**, pp. 67–114.

Petterssen, S., 1959, *On the Influence of Heat Exchanges on Motion and Weather Systems.* Scientific Report No. 10, Contract No. AF19(604)-2179, Dept. of Meteorology, The University of Chicago.

Priestly, C. H. B., 1957, *The Evolution of Energy Gain by the Atmosphere through Contact with the Ground and Ocean.* Scientific Report No. 2, Contract No. AF19(604)-2179, Dept. of Meteorology, The University of Chicago.

Priestly, C. H. B., 1959, Heat conduction and temperature profiles in air and soil, *Journal of the Australian Institute of Agricultural Science,* Vol. 25, pp. 94–107.

Smagorinsky, J., 1953, The dynamical influence of large scale heat sources and sinks on the quasi-stationary mean motions of the atmosphere. *Quart. J. Roy. Met. Soc.,* **97**, pp. 342–366.

Sverdrup, H. U., 1952, *Oceanography for Meteorologists.* George Allen and Unwin Ltd., London, 241 pp.

Wiin-Nielsen, A. C., 1961, On the distribution of temperature relative to height in stationary planetary waves. *Tellus,* **13**, pp. 127–139.

Winston, J. S., 1955, Physical aspects of rapid cyclogenesis in the gulf of Alaska. *Tellus,* **7**, pp. 481-500.